

Original Article

Activation of necroptosis in a rat model of acute respiratory distress syndrome induced by oleic acid

PAN Long^{1,2}, YAO Dun-Chen^{1,2}, YU Yu-Zhong^{1,2}, CHEN Bing-Jun^{1,2}, LI Sheng-Jie^{1,3}, HU Gui-He^{1,2}, XI Chang^{1,2}, WANG Zi-Hui^{1,4}, LI Jian-Hua¹, LONG Jie⁵, TU Yong-Sheng^{1,*}

¹Department of Physiology, School of Basic Sciences; ²The Third Clinical Medical College; ³The First Clinical Medical College; ⁴The Second Clinical Medical College; ⁵Department of Pathology, School of Basic Sciences, Guangzhou Medical University, Guangzhou 511436, China

Abstract: The present study was aimed to investigate the role of necroptosis in the pathogenesis of acute respiratory distress syndrome (ARDS). The rat model of ARDS was induced by intravenous injection of oleic acid (OA), and observed for 4 h. The lung injury was evaluated by arterial blood gas, lung wet-dry weight ratio (W/D) and histological analyses. Simultaneously, bronchoalveolar lavage fluid (BALF) was collected for total and differential cell analysis and total protein determination. Tumor necrosis factor alpha (TNF- α) level in BALF was determined with a rat TNF- α ELISA kit. Expressions of receptor interacting protein kinase 1 (RIPK1), RIPK3 and mixed lineage kinase domain-like protein (MLKL) in lung tissue were determined by Western blot and immunohistochemical staining. The interaction between RIPK1 and RIPK3 was explored by immunoprecipitation. The results showed that, compared with those in control group, total white blood cells count (WBC), polymorphonuclear percentage (PMN%), total protein concentration, TNF- α level in BALF, W/D, and the alveolar-arterial oxygen tension difference (P(A-a)O₂) in OA group were significantly increased at 4 h after OA injection. Western blot and immunostaining further showed remarkably increased expressions of RIPK1, RIPK3 and MLKL in lung tissue from OA group. Additionally, immunoprecipitation results indicated an enforced interaction between RIPK1 and RIPK3 in OA group. Collectively, the TNF- α level in BALF and the RIPK1-RIPK3-MLKL signaling pathway in lung tissue were found to be upregulated and activated with the process of ARDS. These findings implicate that RIPK1/RIPK3-mediated necroptosis plays a possible role in the pathogenesis of ARDS, which may provide a new idea to develop novel drugs for the therapy of ARDS.

Key words: acute respiratory distress syndrome; necroptosis; TNF- α ; receptor interacting protein kinase 1 (RIPK1); RIPK3; mixed lineage kinase domain-like protein

程序性坏死参与油酸诱导的大鼠急性呼吸窘迫综合征的发病过程

潘龙^{1,2}, 姚敦琛^{1,2}, 余雨中^{1,2}, 陈秉钧^{1,2}, 李晟杰^{1,3}, 胡桂和^{1,2}, 奚畅^{1,2}, 王梓晖^{1,4}, 李建华¹, 龙捷⁵, 涂永生^{1,*}

广州医科大学¹基础学院生理教研室; ²第三临床学院; ³第一临床学院; ⁴第二临床学院; ⁵基础学院病理教研室, 广州 511436

摘要: 本研究旨在明确程序性坏死在急性呼吸窘迫综合征(acute respiratory distress syndrome, ARDS)发病中的作用。通过尾静脉注射油酸(oleic acid, OA)制备大鼠ARDS模型, 并观察4 h。通过动脉血气分析、肺干湿重比(lung wet-dry weight ratio, W/D)、肺组织HE染色及肺泡灌洗液(bronchoalveolar lavage fluid, BALF)中总蛋白测定、白细胞计数及分类计数来评估ARDS模

Received 2016-04-28 Accepted 2016-07-22

This work was supported by the National Natural Science Foundation of China (No. 81470205), National College Students' Innovation Entrepreneurship Training Plan Program of China (No. 2015105700010), the Guangzhou Medical University College Students Science and Technology Innovation Project, China (No. 2014A015), the Medical Scientific Research Foundation of Guangdong Province, China (No. A2016382), Guangzhou City-belonged Universities Scientific Research Program, China (No. 2012C130), and the Foundation for Excellent Teachers by Guangzhou Medical University, China.

*Corresponding author. Tel: +86-20-37103213; E-mail: tuys@gzhmu.edu.cn

型。通过ELISA检测BALF中肿瘤坏死因子 α (tumor necrosis factor alpha, TNF- α)水平。通过免疫组化和蛋白免疫印迹观察受体相互作用蛋白激酶1 (receptor interacting protein kinase 1, RIPK1)、RIPK3、mixed lineage kinase domain-like protein (MLKL)在肺组织中的表达水平。通过免疫沉淀观察RIPK1和RIPK3之间的相互作用。结果显示, OA注射4 h后, 与对照组比较, OA组大鼠肺泡-动脉氧分压差 $[P(A-a)O_2]$ 、W/D、BALF中白细胞总数、中性粒细胞比例、蛋白浓度及TNF- α 水平均显著上升, 而氧合指数 (PaO_2/FiO_2) 下降; OA组大鼠肺组织中RIPK1、RIPK3、MLKL表达明显增加, 且RIPK1与RIPK3之间的相互作用显著增强。以上结果表明, 在ARDS的发生、发展过程中, TNF- α 分泌增加, RIPK1/RIPK3/MLKL信号通路被激活并表达上调, 提示程序性坏死可能在ARDS的发病机制中发挥作用, 这可能为治疗ARDS的新药开发提供新思路。

关键词: 急性呼吸窘迫综合征; 程序性坏死; 肿瘤坏死因子 α ; 受体相互作用蛋白激酶1; 受体相互作用蛋白激酶3; MLKL
中图分类号: R363

Acute respiratory distress syndrome (ARDS) is a fulminant disease characterized by pulmonary edema, hypoxemia and decreased pulmonary compliance leading to respiratory failure. Despite advances in the past decades in the knowledge and treatment of ARDS, the mortality remains unacceptably high^[1], ranging from 27% to 45%^[2]. The main pathological characteristics of ARDS include accumulation of neutrophils in the lung microvasculature, interstitium and the alveoli, alterations in the alveolar permeability barrier, deposition of hyaline membrane in the inter-alveolar septa and formation of microthrombi^[2-5]. Damage of the capillary endothelium and alveolar epithelium and subsequent accumulation of protein-rich fluid inside the alveoli, lead to release of pro-inflammatory cytokines such as tumor necrosis factor α (TNF- α)^[3], interleukin-1 (IL-1) and IL-6^[4]. These chemotactic factors from activated macrophages, pulmonary epithelial and endothelial cells activate and recruit neutrophils to sites of inflammation^[5]. Then the activated neutrophils release toxic mediators, such as reactive oxygen species, bioactive lipids, cytokines and proteases, and induce the formation of neutrophil extracellular traps (NETs)^[6]. These cytotoxic molecules induce apoptosis and autophagy, each of which causes tissue injury and cell death, which are characteristic of ARDS^[4, 7]. It is interesting to explore whether necroptosis is induced by these cytotoxic molecules.

Necroptosis is a recently discovered programmed necrosis, regulated by receptor interacting protein kinase 1 (RIPK1), RIPK3 and the pseudokinase mixed lineage kinase domain-like protein (MLKL) after death signal stimulation^[8-10]. Necroptosis was regarded as a drug-targetable contributor to necrotic injury in many animal models of human diseases, including ischemia-reperfusion injuries (brain, kidney), neurodegenerative diseases and inflammation. Therefore, blocking the kinase activity of RIPK1 by drugs can inhibit the activation of

necroptosis, and may provide therapeutic benefits for the treatment of human diseases characterized by necrosis and inflammation. Necroptosis and RIPK1-RIPK3 necrosome formation can be induced by several factors, mainly including TNF- α ^[11-13]. Interestingly, TNF- α is elevated in active lesions, the serum and bronchoalveolar lavage fluid (BALF) of ARDS patients^[6]. Cytokines such as TNF- α and interleukin are important mediators in the development of ARDS, contributing to augmented vascular permeability and organ dysfunction^[4]. Simultaneously, necroptosis has been shown to be implicated in the pathogenesis of various lung disease models^[14-16]. In consideration that ARDS is an inflammation disease, and inflammation caused by necroptosis contributes to tissue damage^[17], but the relationship between necroptosis and ARDS remains unknown.

Thus, in the present study, we investigate the role of RIPK1/RIPK3-mediated necroptosis in ARDS and want to demonstrate whether RIPK1/RIPK3-mediated necroptosis is activated during ARDS, which will present new evidence for the involvement of RIPK1/RIPK3-mediated necroptosis in the pathogenesis of ARDS.

1 MATERIALS AND METHODS

1.1 Rat model of ARDS

This study was approved by Animal Care and Use Committee, Guangzhou Medical University. All the animal experimental procedures were conducted in line with the “Guide for the Care and Use of Laboratory Animals” of China. Male Sprague-Dawley rats, 6–8 weeks old, were purchased from Guangdong Medical Laboratory Animal Center (Foshan, Guangdong, China). Rats were randomly allocated to control group and oleic acid (OA) group. Each animal in OA group was injected intravenously with pure OA at dose of 100 μ L/kg. Control animals received an injection of an equal volume of saline.

1.2 Evaluation parameters of ARDS

At 4 h after injection of OA, the arterial blood specimens obtained from carotid artery were analyzed for PaO₂, PaCO₂, and pH using automatic blood gas Analyzer ABL800 (Radiometer, Copenhagen, Denmark). Fraction of inspiration O₂ (FiO₂) was regarded as 21% because all the rats were placed in the air. The PaO₂/FiO₂ ratio was the ratio of PaO₂ to FiO₂. The alveolar-arterial oxygen tension difference (P(A-a)O₂) was calculated using the standard alveolar gas equation with an assumed respiratory quotient of 1.0.

The inferior lobe of right lung was excised and weighed immediately. Lung tissues were dried in an oven at 60 °C for 72 h and reweighed. Wet/dry weight ratio (W/D) was calculated to assess lung edema.

Total and differential cell analysis and total protein assay of BALF were performed as previously described^[18]. Bronchoalveolar lavage was performed after the trachea was isolated by blunt dissection. A small caliber tube was inserted into the airway. Three volumes of 3.0 mL of cold PBS were sequentially infused in and out of the airways after right lung was ligated. In every cycle, the same volume (3.0 mL) was recovered from each animal. Total leukocyte counts were performed by optical microscopy in Neubauer chambers after diluting BALF samples in Türk solution (2% acetic acid). Differential leukocyte counts were determined in cytocentrifuged smears stained with May-Grunwald-Giemsa. The BALF total protein in the supernatant was determined by BCA Protein Assay Kit (Beyotime, Haimen, China) according to the manufacturer's instructions.

1.3 Histological and immunohistochemical studies

Hematoxylin and eosin (H&E) and immunohistochemistry staining was performed as our previous experiments with minor modification^[19]. The rest of the right lung was first perfused with 1 mL of 10% formalin via the trachea to inflate and fix the lung tissue. The trachea was tied off using suture thread, and the fixed lung was isolated and stored in 4% paraformaldehyde until further processing. Fixed organs were dehydrated, and embedded in paraffin, and 5- μ m sections were cut for H&E and immunohistochemistry staining. Briefly, sections were heated and deparaffinized. All incubations were performed in a humidified chamber at room temperature after retrieval. After endogenous peroxidase was blocked and antigen was retrieved, slides were then incubated with 5% normal goat serum in PBS sup-

plemented with 1% BSA for 30 min to prevent non-specific binding of antibodies. After blocking, the sections were incubated at 4 °C overnight with the following diluted primary antibodies: anti-RIPK1 (1:50 dilution; Santa Cruz Biotechnology, Dallas, USA), anti-RIPK3 (1:200 dilution; Sigma-Aldrich, Saint Louis, USA), and anti-MLKL (1:200 dilution; Abcam, Cambridgeshire, UK). Subsequently, the sections were incubated with HRP-conjugated secondary goat anti-rabbit antibody (1:500 dilution; Maixin, Fujian, China) for 60 min at 37 °C. Immunoreactivity was detected with the DAB substrate kit (Maixin, Fujian, China), and the sections were counterstained with hematoxylin. Photos were taken using an optical microscope (Nikon eclipse 80i, Tokyo, Japan).

1.4 ELISA assay for measurement of TNF- α in BALF

The fluid was centrifuged at 1 500 r/min at 4 °C for 10 min to remove the cells. The cell-free supernatant was divided into several aliquots and stored at -80 °C until assayed. The concentration of TNF- α was determined by ELISA (Elabscience, Wuhan, China). Fresh samples were used for the ELISA according to the manufacturer's specification. The optical density of each well was read at 450 nm using a microplate reader Multiskan GO 1.00.38 (Thermo Scientific, Massachusetts, USA). "Curve Expert 1.3" was used to make a standard curve and calculate samples concentration of TNF- α .

1.5 Immunoprecipitation and Western blot analysis

The left lung was immediately removed and homogenized with RIPA buffer containing 50 mmol/L Tris (pH 7.4), 150 mmol/L NaCl, 1% Triton X-100, 1% sodium deoxycholate, 0.1% SDS, sodium orthovanadate, sodium fluoride, EDTA, and leupeptin. The lysates were centrifuged at 15 000 g for 5 min at 4 °C, and the supernatant was removed. For RIPK1 immunoprecipitation, 2 μ g rabbit anti-RIPK1 antibody was added in 1 mL lysates (Santa Cruz Biotechnology, Dallas, USA) and incubated overnight at 4 °C. Then, the lysates were incubated with 40 μ L Protein A+G Agarose (Beyotime, Haimen, China) at 4 °C for 3 h with gentle rocking. Beads were washed five times with lyses buffer, and the proteins were eluted by boiling in 1 \times SDS-PAGE loading buffer before Western blot.

Western blot was performed as previously described in our lab^[20]. Briefly, the lysates were loaded and electrophoresed on 10% polyacrylamide-SDS gels and then transferred to a nitrocellulose membrane. After blocking with 5% milk in TBST for 1 h, the membrane was

incubated overnight at 4 °C with rabbit anti-RIPK1 (1:1 000 dilution; Santa Cruz Biotechnology, Dallas, TX, USA), anti-RIPK3 (1:2 000 dilution; Sigma-Aldrich, Saint Louis, USA), anti-MLKL (1:2 000 dilution; Abcam, Cambridgeshire, UK), or mouse anti- β -actin antibodies (1:5 000 dilution; Cell Signaling Technology, Beverly, USA). After 1 h of incubation at room temperature with the appropriate HRP-linked anti-rabbit or anti-mouse secondary antibody (Cell Signaling Technology, Beverly, USA), the blots were incubated with chemiluminescence substrates (Pierce Biotechnology, Rockford, USA) and then were visualized by gel image system.

1.6 Statistics

Quantitative results were expressed as mean \pm SD. Statistical significance of differences between means was assessed using two independent sample *t*-test using SPSS 16.0 software program. A value of $P < 0.05$ was considered to be statistically significant.

2 RESULTS

2.1 ARDS was induced at 4 h after OA injection

We combined PaO₂/FiO₂ ratio, P(A-a)O₂, W/D, BALF

protein concentration, BALF leukocytes, polymorphonuclear percentage (PMN%) and H&E staining of lung tissues to evaluate the lung injury after injection of OA. The PaO₂/FiO₂ ratio in the OA group significantly decreased compared with that in the saline control group at 4 h after OA infusion (Fig. 1A). In contrast to the PaO₂/FiO₂ ratio, P(A-a)O₂ was markedly increased in the OA group compared with that in the saline control group (Fig. 1B). These data indicated pulmonary ventilation dysfunction in the OA group. Then we used W/D and protein concentration in BALF to evaluate alveolar edema and vascular permeability. The W/D and protein concentration in BALF were prominently increased in OA group compared with those in saline group (Fig. 1C, D). In addition, we examined the amount of leukocytes in BALF to see inflammatory cell infiltration in the lung tissue. Compared with those in the saline control group, the total amount of leukocytes (Fig. 1E) and PMN% (Fig. 1F) in BALF from the OA group were dramatically higher, which indicates more inflammatory cell infiltration in the lung tissue after OA administration. Lastly, we used H&E staining to evaluate the lung injury. At 4 h after injecting OA, there were obvi-

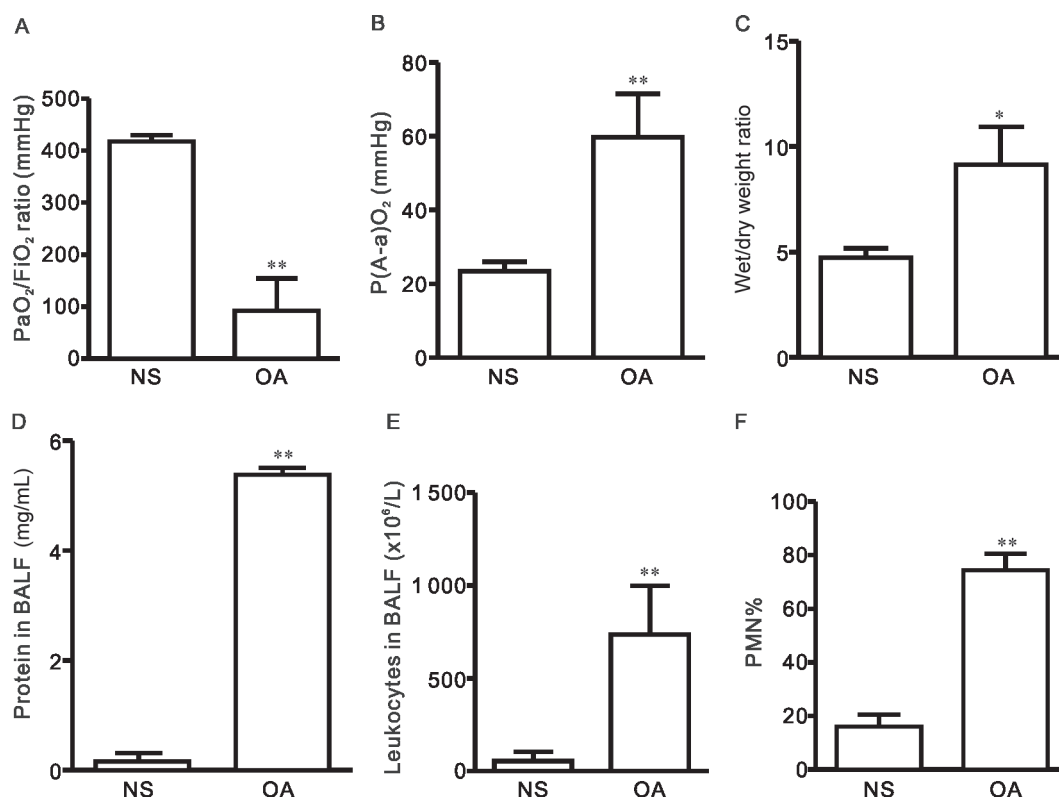


Fig. 1. Changes of PaO₂/FiO₂ ratio (A), P(A-a)O₂ (B), W/D (C), BALF protein concentration (D), BALF leukocytes (E), PMN% (F) in rat model of ARDS induced by OA. These data demonstrated lung edema and inflammation. NS: normal saline. OA: oleic acid. The results are means \pm SD from 7 different animals. * $P < 0.05$, ** $P < 0.01$ compared to control (NS).

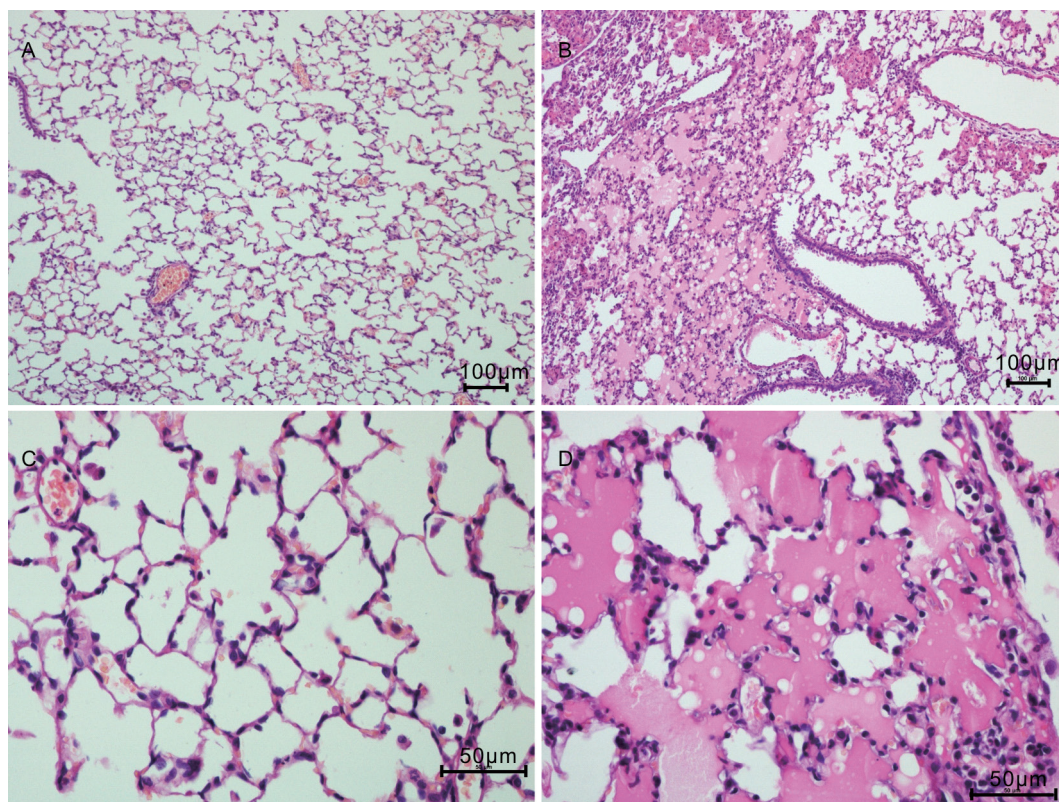


Fig. 2. Hematoxylin and eosin staining of lung tissues. Sterile saline (A, C) and OA (B, D) were correspondingly injected i.v. at 4 h before the collection of the lungs. OA induced obvious lung pathological changes that are similar to clinical ARDS, such as interstitial and alveolar edema and leukocytes infiltration. Scale bar, 100 μm (A, B); Scale bar, 50 μm (C, D).

ous pathological changes in the lung, such as marked alveolar edema, vascular congestion, intravascular coagulation, alveolar hemorrhage, alveolar walls disruption and leukocytes infiltration (Fig. 2B, D). Collectively, the above data illustrated that the rat model of ARDS was successfully induced by the injection of OA.

2.2 RIPK1, RIPK3 and MLKL mediated-necroptosis was found in the rat lung tissues of ARDS associated with increased TNF- α in BALF

Our results showed that ARDS was accompanied by increased protein expressions of RIPK1, RIPK3 and MLKL (Fig. 3B, C) detected by Western blot at 4 h after OA infusion, as well as enhanced TNF- α level in BALF detected by ELISA (Fig. 3A). The formation of necrosome containing RIPK1 and RIPK3 is unique for the initiation of necroptosis. Thus, we further investigated the recruitment of RIPK3 to RIPK1 by immunoprecipitation to ascertain this necroptosis pathway is activated. Our results showed that the interaction between RIPK1 and RIPK3 was greatly enhanced in OA-treated rats (Fig. 3D, E). Finally, we used immuno-

histochemistry staining to further explore the expression pattern of RIPK1, RIPK3 and MLKL in the lung tissues. Staining results showed that the three proteins in the lung tissue from the OA group (Fig. 3I, J, K) were significantly higher than those from control groups (Fig. 3F, G, H). Together, increased expressions of RIPK1, RIPK3 and MLKL, and interaction between RIPK1 and RIPK3 indicated necroptosis occurred during ARDS, suggesting that necroptosis could be involved in ARDS.

3 DISCUSSION

Necroptosis was found to be involved in the pathogenesis of many diseases [12, 21–23]. However, the role of necroptosis in ARDS remains unclear. Therefore, it is necessary to investigate the relationship between necroptosis and ARDS. Here, we found that the TNF- α level was increased in BALF from ARDS rats. Additionally, the enhanced activation and expression of RIPK1/RIPK3/MLKL signaling pathway was accompanied with ARDS, which implicates necroptosis is possibly

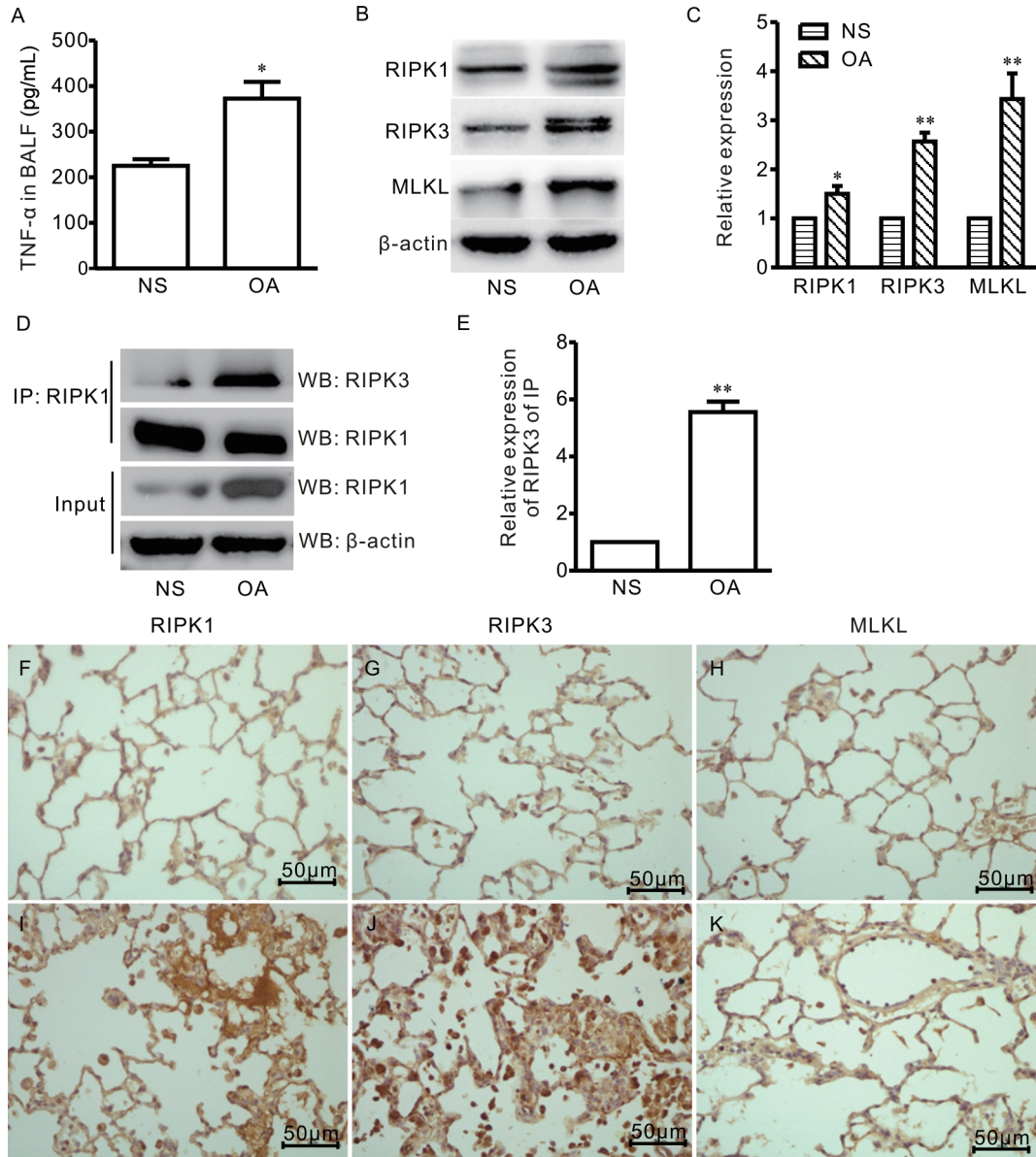


Fig. 3. Oleic acid (OA)-induced rat model of ARDS was associated with increased TNF- α and necroptosis through RIPK1, RIPK3 and MLKL signal pathway. *A*: TNF- α in BALF was increased by OA injection. *B* (bands) and *C* (quantification): Western blot results showed that RIPK1, RIPK3 and MLKL protein levels were enhanced in lung tissues from OA-treated rats. *D* (bands) and *E* (quantification): Immunoprecipitation results showed that the interaction between RIPK1 and RIPK3 was strikingly enhanced in OA-treated rats. *F–K*: Slides of lung tissues from saline control (*F, G, H*) and OA (*I, J, K*) rats were used to examine expressions of RIPK1, RIPK3, MLKL by immunohistochemistry staining. Scale bar, 50 μ m. TNF- α results are means \pm SD from 7 different animals. Western blot experiments were repeated at least three times. * $P < 0.05$, ** $P < 0.01$ compared to control (NS).

involved in the pathogenesis of ARDS.

Above all, rat model of ARDS produced by injection of OA was evaluated by PaO₂/FiO₂ ratio, W/D, protein concentration in BALF, BALF leukocytes and H&E staining of lung tissue. Our results showed typical pathological changes in the rat lung resembling ARDS, such as marked alveolar edema, alveolar hemorrhage, alveolar walls disruption and leukocytes infiltration.

The TNF- α in BALF was significantly increased in ARDS rats. These data indicated the injection of OA induced lung injury and inflammation.

Then we continued to investigate whether OA-induced lung injury and inflammation was associated with necroptosis. We found that the expressions of RIPK1, RIPK3 and MLKL (markers for necroptosis) were significantly enhanced in the lung. We further

demonstrated that the interaction of RIPK1 and RIPK3 was prominently enhanced in the lung tissues of ARDS rats. Activation of necroptosis requires cross-phosphorylation of RIPK1 and RIPK3, utilizing Ser/Thr kinase domains of both proteins^[10]. And RIPK3 recruits and phosphorylates pseudokinase MLKL on Thr357/Ser358, which serves as a critical gateway to necroptosis execution^[24–26]. Once oligomerized, MLKL was transferred from the cytoplasm to intracellular and plasma membranes, where the necrosome directly disrupts membrane integrity by forming pores, resulting in necrotic death^[27]. Therefore, it indicates that necroptosis through RIPK1/RIPK3/MLKL signaling occurs in OA-induced ARDS rat. Interestingly, it has been reported that RIPK1 can promote the production of TNF- α ^[28]. While other recent evidence suggests that initiation of necroptosis is due to stimulation of TNF- α signaling^[13, 29]. Therefore, increased level of TNF- α in BALF may lead to necroptosis or further increase by necroptosis in OA-induced ARDS rat. However, cause and effect relationship between TNF- α and necroptosis in ARDS needs to be further studied.

In conclusion, our study is the first report indicating the involvement of necroptosis in ARDS induced by OA in rats. TNF- α in BALF and RIPK1/RIPK3/MLKL signal pathway in lung tissue were activated and up-regulated with the development of ARDS. These data suggest that pathogenesis of ARDS might involve necroptosis, including RIPK1, RIPK3 and MLKL, which may provide a novel therapeutic approach to the treatment of ARDS. Further studies are needed to investigate whether the inhibition of necroptosis can alleviate or even cure ARDS.

REFERENCES

- 1 Walkey AJ, Sumner R, Ho V, Alkana P. Acute respiratory distress syndrome: epidemiology and management approaches. *Clin Epidemiol* 2012; 4: 159–169.
- 2 Ranieri VM, Rubenfeld GD, Thompson BT, Ferguson ND, Caldwell E, Fan E, Camporota L, Slutsky AS. Acute respiratory distress syndrome: the Berlin Definition. *JAMA* 2012; 307(23): 2526–2533.
- 3 Windsor AC, Walsh CJ, Mullen PG, Cook DJ, Fisher BJ, Blocher CR, Leeper-Woodford SK, Sugerman HJ, Fowler AA 3rd. Tumor necrosis factor-alpha blockade prevents neutrophil CD18 receptor upregulation and attenuates acute lung injury in porcine sepsis without inhibition of neutrophil oxygen radical generation. *J Clin Invest* 1993; 91(4): 1459–1468.
- 4 Fujishima S. Pathophysiology and biomarkers of acute respiratory distress syndrome. *J Intensive Care* 2014; 2(1): 32.
- 5 Wilhelmssen K, Mesa KR, Prakash A, Xu F, Hellman J. Activation of endothelial TLR2 by bacterial lipoprotein upregulates proteins specific for the neutrophil response. *Innate Immun* 2012; 18(4): 602–616.
- 6 Windsor AC, Mullen PG, Fowler AA, Sugerman HJ. Role of the neutrophil in adult respiratory distress syndrome. *Br J Surg* 1993; 80(1): 10–17.
- 7 Pierrakos C, Karanikolas M, Scolletta S, Karamouzou V, Vellissaris D. Acute respiratory distress syndrome: pathophysiology and therapeutic options. *J Clin Med Res* 2012; 4(1): 7–16.
- 8 Hitomi J, Christofferson DE, Ng A, Yao J, Degterev A, Xavier RJ, Yuan J. Identification of a molecular signaling network that regulates a cellular necrotic cell death pathway. *Cell* 2008; 135(7): 1311–1323.
- 9 He S, Wang L, Miao L, Wang T, Du F, Zhao L, Wang X. Receptor interacting protein kinase-3 determines cellular necrotic response to TNF-alpha. *Cell* 2009; 137(6): 1100–1111.
- 10 Cho YS, Challa S, Moquin D, Genga R, Ray TD, Guildford M, Chan FK. Phosphorylation-driven assembly of the RIP1-RIP3 complex regulates programmed necrosis and virus-induced inflammation. *Cell* 2009; 137(6): 1112–1123.
- 11 Vercammen D, Vandenabeele P, Beyaert R, Declercq W, Fiers W. Tumour necrosis factor-induced necrosis versus anti-Fas-induced apoptosis in L929 cells. *Cytokine* 1997; 9(11): 801–808.
- 12 Ofengeim D, Ito Y, Najafav A, Zhang Y, Shan B, DeWitt JP, Ye J, Zhang X, Chang A, Vakifahmetoglu-Norberg H, Geng J, Py B, Zhou W, Amin P, Berlink Lima J, Qi C, Yu Q, Trapp B, Yuan J. Activation of necroptosis in multiple sclerosis. *Cell Rep* 2015; 10(11): 1836–1849.
- 13 Vandenabeele P, Declercq W, Van Herreweghe F, Vanden Berghe T. The role of the kinases RIP1 and RIP3 in TNF-induced necrosis. *Sci Signal* 2010; 3(115): re4.
- 14 Zhao H, Ning J, Lemaire A, Koumpa FS, Sun JJ, Fung A, Gu J, Yi B, Lu K, Ma D. Necroptosis and parthanatos are involved in remote lung injury after receiving ischemic renal allografts in rats. *Kidney Int* 2015; 87(4): 738–748.
- 15 Kitur K, Parker D, Nieto P, Ahn DS, Cohen TS, Chung S, Wachtel S, Bueno S, Prince A. Toxin-induced necroptosis is a major mechanism of *Staphylococcus aureus* lung damage. *PLoS Pathog* 2015; 11(4): e1004820.
- 16 Jiang Y, Shan S, Chi L, Zhang G, Gao X, Li H, Zhu X, Yang J. Methyl methanesulfonate induces necroptosis in human lung adenoma A549 cells through the PIG-3-reactive oxygen species pathway. *Tumour Biol* 2016; 37(3): 3785–3795.
- 17 Newton K, Manning G. Necroptosis and Inflammation. *Annu*

- Rev Biochem 2016; 85: 743–763.
- 18 Goncalves-de-Albuquerque CF, Burth P, Silva AR, de Moraes IM, de Jesus Oliveira FM, Santelli RE, Freire AS, Bozza PT, Younes-Ibrahim M, de Castro-Faria-Neto HC, de Castro-Faria MV. Oleic acid inhibits lung Na/K-ATPase in mice and induces injury with lipid body formation in leukocytes and eicosanoid production. *J Inflamm (Lond)* 2013; 10(1): 34.
- 19 Tang FC, Wang HY, Ma MM, Guan TW, Pan L, Yao DC, Chen YL, Chen WB, Tu YS, Fu XD. CyPA-CD147-ERK1/2-cyclin D2 signaling pathway is upregulated during rat left ventricular hypertrophy. *Acta Physiol Sin (生理学报)* 2015; 67(4): 393–400.
- 20 Tu YS, Kang XL, Zhou JG, Lv XF, Tang YB, Guan YY. Involvement of Chk1-Cdc25A-cyclin A/CDK2 pathway in simvastatin induced S-phase cell cycle arrest and apoptosis in multiple myeloma cells. *Eur J Pharmacol* 2011; 670(2–3): 356–364.
- 21 Zhou W, Yuan J. Necroptosis in health and diseases. *Semin Cell Dev Biol* 2014; 35: 14–23.
- 22 Su X, Wang H, Kang D, Zhu J, Sun Q, Li T, Ding K. Necrostatin-1 ameliorates intracerebral hemorrhage-induced brain injury in mice through inhibiting RIP1/RIP3 pathway. *Neurochem Res* 2015; 40(4): 643–650.
- 23 Rosenbaum DM, Degtarev A, David J, Rosenbaum PS, Roth S, Grotta JC, Cuny GD, Yuan J, Savitz SI. Necroptosis, a novel form of caspase-independent cell death, contributes to neuronal damage in a retinal ischemia-reperfusion injury model. *J Neurosci Res* 2010; 88(7): 1569–1576.
- 24 Murphy JM, Czabotar PE, Hildebrand JM, Lucet IS, Zhang JG, Alvarez-Diaz S, Lewis R, Lalaoui N, Metcalf D, Webb AI, Young SN, Varghese LN, Tannahill GM, Hatchell EC, Majewski IJ, Okamoto T, Dobson RC, Hilton DJ, Babon JJ, Nicola NA, Strasser A, Silke J, Alexander WS. The pseudokinase MLKL mediates necroptosis via a molecular switch mechanism. *Immunity* 2013; 39(3): 443–453.
- 25 Sun L, Wang H, Wang Z, He S, Chen S, Liao D, Wang L, Yan J, Liu W, Lei X, Wang X. Mixed lineage kinase domain-like protein mediates necrosis signaling downstream of RIP3 kinase. *Cell* 2012; 148(1–2): 213–227.
- 26 Wu J, Huang Z, Ren J, Zhang Z, He P, Li Y, Ma J, Chen W, Zhang Y, Zhou X, Yang Z, Wu SQ, Chen L, Han J. Mkl1 knockout mice demonstrate the indispensable role of Mkl1 in necroptosis. *Cell Res* 2013; 23(8): 994–1006.
- 27 Wang H, Sun L, Su L, Rizo J, Liu L, Wang LF, Wang FS, Wang X. Mixed lineage kinase domain-like protein MLKL causes necrotic membrane disruption upon phosphorylation by RIP3. *Mol Cell* 2014; 54(1): 133–146.
- 28 Christofferson DE, Li Y, Hitomi J, Zhou W, Upperman C, Zhu H, Gerber SA, Gygi S, Yuan J. A novel role for RIP1 kinase in mediating TNF α production. *Cell Death Dis* 2012; 3: e320.
- 29 Moriwaki K, Bertin J, Gough PJ, Orłowski GM, Chan FK. Differential roles of RIPK1 and RIPK3 in TNF-induced necroptosis and chemotherapeutic agent-induced cell death. *Cell Death Dis* 2015; 6: e1636.